ACS Catalysis

Research Article

pubs.acs.org/acscatalysis

Oxyhalogenation of Activated Arenes with Nanocrystalline Ceria

Antonio Leyva-Pérez,*[,†] Diego Cómbita-Merchán,[†] Jose R. Cabrero-Antonino,[†] Saud I. Al-Resayes,[‡] and Avelino Corma*[,†,‡]

[†]Instituto de Tecnología Química. Universidad Politécnica de Valencia, Consejo Superior de Investigaciones Científicas, Avenida de los Naranjos s/n, 46022 Valencia, Spain

[‡]Chemistry Department, College of Science, King Saud University, B.O. box 2455, Riyadh 11451, Saudi Arabia

Supporting Information

ABSTRACT: Arenes can be chlorinated, brominated, and iodinated in the presence of CeO_2 nanoparticles under aerobic conditions. In a biomimetic approach, active electrophilic halogen species are generated from either organic or inorganic halogen compounds and are trapped by arenes. This C−H transformation can be applied to the synthesis of naturally occurring products.

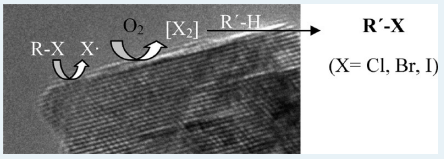

KEYWORDS: *nanocrystalline ceria, organohalides, oxidative halogenation, electrophilic aromatic substitution, molecular oxygen as oxidant*

INTRODUCTION

Halogenation of hydrocarbons is an important process in industry and also in nature.[1] This reaction is generally performed with common halogenating agents, such as simple dihalogens X_2 (X: F, Cl, Br, I) as well as organohalides having an activated $X^{\delta+}$ atom, that is, thionyl halides and *N*-halosuccimides. Overall, the halogenation process requires the use of stoichiometric amounts of hazardous unstable chemicals, particularly in the case of F_2 and Cl_2, which complicates the feasibility of the transformation. An alternative reaction procedure involves the bioinspired oxidative halogenation.[2] In this methodology, the $X^{\delta+}$ species is generated in situ by oxidation of a simple salt (Y^+X^-; Y: H, alkaline cation, R_4N, ...) with peroxides (typically H_2O_2) in the presence or not of a catalyst.[3,4] In addition, the oxyhalogenation gives, in contrast to classical procedures, preferential access to bromo- and iodoarenes, which engage easily in metal-catalyzed cross-coupling reactions. Nevertheless, the oxyhalogenation reaction still needs unstable reagents, such as mineral acids or peroxides and requires highly polar solvents (typically alcohols, acetonitrile, ionic liquids, or water) to dissolve the oxidant and the acid/salt.

Ceria (CeO_2) is a robust and accessible solid that has found important applications in industry[5] and presents potential uses in biological systems.[6] The nonstoichiommetric nature of CeO_{2-x} generates oxygen vacancies and reactive oxygen species (ORS) that allow high oxygen mobility. The oxygen vacancies can be occupied by other electronegative atoms (i.e. halogens), and it has been reported that ceria decomposes chlorinated solvents at high temperatures by progressive incorporation of the chloride atom onto the oxide structure (eq 1).[7−12]

$$2CeO_2 + 2CCl_4 \xrightarrow{>300\ ^\circ C} 2CeCl_3 + 2CO_2 + Cl_2 \quad (1)$$

$$Ce^{4+} + X^- \rightarrow Ce^{3+} + (1/2)X_2 \qquad X = Cl, Br, I \quad (2)$$

$$Ce^{3+} + O_2 \rightarrow CeO_2 \quad (3)$$

According to eq 1, significant amounts of active halogenating species (X_2) are generated from simple organic halides. If one could operate the process at much lower temperatures, the interception of the X_2 species by electron-rich hydrocarbons would give a formal oxyhalogenation reaction with the organic halide acting as solvent/reagent source. It was early reported[13] that $CeCl_3$ is beneficial during the copper-on-alumina-catalyzed oxychlorination of benzene, but in this case, the role of cerium is just to reoxidize the copper. With only cerium, the process would be feasible, since the redox potential of the pair Ce^{4+}/Ce^{3+} (1.44 eV) is higher than that of Cl, Br, and I halides (1.36, 1.07, and 0.54 eV, respectively), and fluoride (2.87 eV) is too high to be oxidized by CeO_2 (eq 2). So if, after transferring the halide, we could reoxidize the Ce^{3+} left behind (eq 3) and the two processes would take place in a continuous mode, CeO_2 could act as a catalyst for the oxidative halogenation of arenes with O_2 without additional metals. Overall, this approach would imply the generation of halonium species from organic halides[14] and oxygen.[15]

RESULTS AND DISCUSSION

Nanocrystalline Ceria As Halogen Activator. Activation of the halogen requires the presence of reactive oxygen species (ORS),[16] which are directly related to the vacancies in the ceria structure. The nonstoichiometry of cerium oxide is enhanced in high surface area materials, since Ce^{3+} is stabilized at the boundaries of the solid and, therefore, the Ce^{3+}/Ce^{4+} ratio increases. A particularly active material is nanocrystalline ceria (n-CeO_2),[16b] having a surface area ~120 $m^2\ g^{-1}$ and particle size <10 nm (Figure 1).

Received: July 4, 2012
Revised: December 13, 2012
Published: December 17, 2012

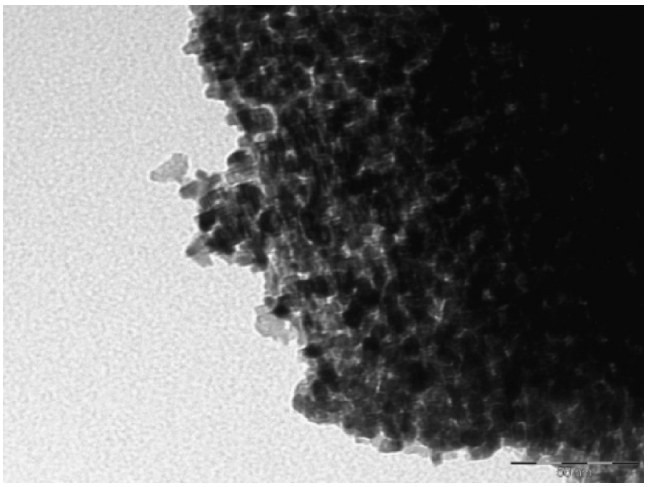

Figure 1. Transmission electron microscopy (TEM) image of nanocrystalline ceria. Average particle size: 8.8 nm.

To study the halogen activation, 1-bromo-3-chloropropane **1** was reacted with catalytic amounts of nanocrystalline ceria under strict anaerobic conditions (argon atmosphere) to avoid any competition of oxygen for vacancies in the solid (Scheme 1). The release of halogen to the medium was detected by the formation of the corresponding homohalogenated products **2** and **3** after halogen exchange.

Scheme 1. Halogen Exchange of 1 in the Presence of a Catalytic Amount of Nanocrystalline Ceria under Anaerobic Conditions

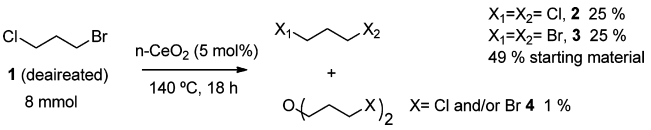

The result shows that monatomic Cl and Br species are, indeed, generated in the presence of nanocrystalline ceria, triggering the statistical formation of the three dihalogenated compounds, **1**–**3**. Significant amounts of the three different ethers **4** were also detected, which infers the participation of ORS. These species are reported to be superoxide or even peroxide radicals,[17] and the halogen exchange is unaffected by the presence of molecular oxygen (see below Figure 3A), by the addition of 4-*tert*-butyl catechol (2 equiv), or by running the reaction in the dark, which suggests that the halide formation is inherent to the basicity of the nanocrystalline ceria. To check this hypothesis, six nano-oxides having different basicities were used as catalysts (Figure 2A). The results indicate that the more basic the material, the higher the halogen exchange rate is, nanomagnesia being the most active material. We can then conclude that the activity of nanocrystalline ceria for halide release is related to the basic sites of the catalyst and the halogen exchange is not affected by the presence of oxygen.

Oxidative Halogenation of Activated Arenes with Organic Halides under Aerobic Conditions. After observing that nanocrystalline ceria generates free halides from **1**, we proceeded to include also the activated arene 1,3,5-trimethoxybenzene **5** in the reaction medium (Scheme 2).

Scheme 2. Halogenation of 1,3,5-Trimethoxybenzene 5 with 1 in the Presence of Nanocrystalline Ceria under Anaerobic or Aerobic Conditions

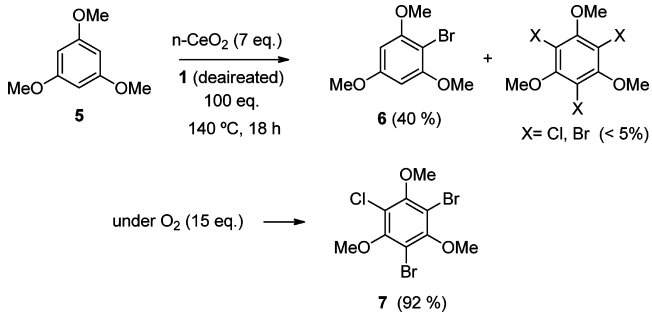

Monobrominated arene **6** was obtained in moderate yield, together with small amounts of polyhalogenated compounds, but the halogenation was significantly accelerated under an atmosphere of molecular oxygen (6 bar), achieving the chlorodibromo adduct **7** in excellent yield and selectivity. The possible Friedel–Crafts alkylation does not compete, since only traces of alkylated arene were found. These halogenated phloroglucinols and derivatives are an important class of natural products with biological activity (see representative examples in Supporting Information Figure S1).[1,18–21]

It was checked again that the presence of oxygen does not affect the halogen exchange (Figure 3A) but, on the contrary, it has a positive role on the halogenation of **5** (Figure 3B). The results in Figure 3 show that the initial rate of halide release is independent of the partial pressure of O_2 while the rate of halogenation clearly increases. In other words, the oxidative halogenation proceeds slowly in the presence of argon and accelerates in the presence of oxygen, whereas halogen exchange does not, and therefore, the latter follows a nonradical mechanism.

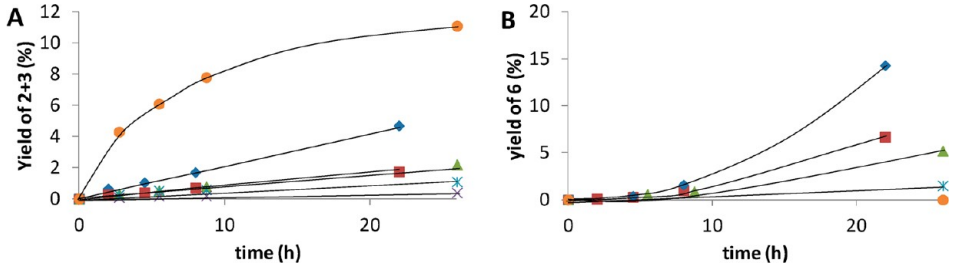

Figure 2. Time–yield plot for the halogen exchange of deaereated 1-bromo-3-chloropropane **1** (A, 40 mmol) or for the halogenation of 1,3,5-trimethoxybenzene **5** (B, 0.125 mmol) under argon at 140 °C in the presence of 0.92 mmol of nanomagnesia (○) or 0.46 mmol of nanocrystalline ceria (<10 nm, ◊), nanoceria (<25 nm, □), nanoceria–zirconia (Δ), nanotitania (*), and nanozirconia (×). For the reaction equation, see Scheme 2.

dx.doi.org/10.1021/cs300644s | *ACS Catal.* 2013, 3, 250–258

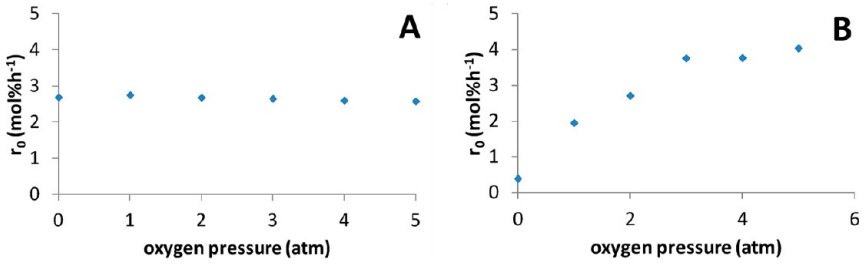

Figure 3. Plot of the concentration initial rate for the halogen exchange of deaereated 1-bromo-3-chloropropane **1** (A) or for the halogenation of 1,3,5-trimethoxybenzene **5** (B) when increasing the oxygen pressure at 140 °C. For the reaction equation, see Scheme 2.

In addition, very small amounts of ethers **4** plus the corresponding alcohols (<0.1 mol % with respect to **1**) were detected during the halogenation of **5**, which suggests that molecular oxygen could play a double role: (1) regenerating the ORS on nanocrystalline ceria or (2) triggering the decomposition of minor byproducts. To have more information on this, the consumption of oxygen was measured while the reaction was monitored by ^{1}H NMR and GC/MS (Figure 4).

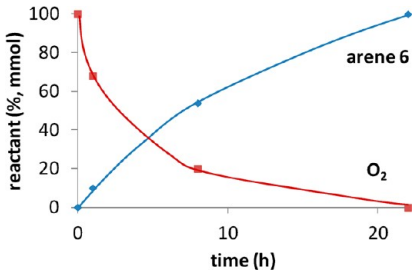

Figure 4. Time−yield plot for the oxygen consumption and the halogenation of 1,3,5-trimethoxybenzene **5** (0.62 mmol) with **1** (7.6 mmol) in the presence of nanocrystalline ceria (0.46 mmol, ~7 mol % with respect to **1**, 0.7 equiv with respect to **5**) under an atmosphere of oxygen (0.9 mmol, 6 bar) at 140 °C, in a reactor equipped with a manometer. Percentages are with reference to **5**.

After an initial strong adsorption of oxygen by nanocrystalline ceria, 1 mol of oxygen per mol of **5** was consumed. This result can be explained by assuming that O_2 is playing a double role, as an oxidant and as a base. The halogenated arene **6** and the halogenated solvents **1**−**3** are the only products found in either ^{1}H NMR or GC/MS analyses, which suggests that halogenation byproducts, such as water, monohalogenated propane[22] or CO_2, are volatiles. To check this, the gaseous phase of the reaction was analyzed by means of GC/MS. It was found that, even at short reaction times (2 h), carbon dioxide was the main component of the gas phase, together with minor amounts of methanol and acetone, independently of the solvent employed, 1,2-dichlorobenzene or 1,3-dibromopropane (see Supporting Information Scheme S1). For the latter, as the reaction further proceeded, methanol was consumed, and methyl bromide was formed, which suggests that HBr was also formed during the reaction and was converted to methyl bromide from the alcohol. This would explain the absence of water in the liquid phase, since the H removed from the arene would pass to the gas phase as HX and only then would evolve to water.

When the six solid catalysts were tested and the oxidative halogenation reaction was analyzed (see Figure 2B), it was clear that only cerium redox materials gave some conversion. Moreover, the introduction of a radical scavenger (4-*tert*-butyl catechol) inhibits the oxidative halogenation reaction. These results indicate that halide release and oxidation by nanocrystalline ceria are two different processes that proceed through a different mechanism. To gain further insight into the mechanism of oxidative halogenation of arenes with cerium oxide, the deuterated arene **5**-d_3 was prepared[23] and tested in the presence of nanocrystalline ceria under aerobic conditions (Figure 5).

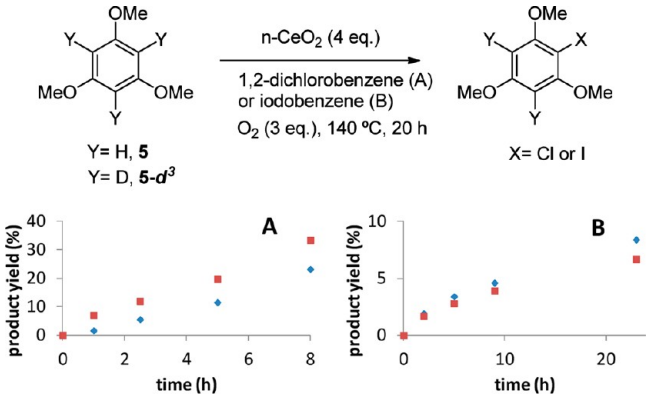

Figure 5. Time−yield plot for the halogenation of 1,3,5-trimethoxybenzene **5** (◊, 0.32 mmol) or the corresponding deuterated compound **5**-d_3 (□) in 0.75 mL of *ortho*-dichlorobenzene (A) or iodobenzene (B) in the presence of nanocrystalline ceria (1.2 mmol) under an atmosphere of oxygen (0.9 mmol, 6 bar) at 140 °C. Calculated KIEs: 0.63 (Cl), 1.19 (I).

The results from Figure 5A show an inverse kinetic isotopic effect (KIE, K_H/K_D = 0.63) for chlorination, which is typical of electrophilic aromatic substitutions (no H-breaking at the transition step).[24,25] In addition, a very small KIE was observed for iodination (Figure 5B), which also supports an electrophilic pathway. It must be noted that no other byproducts from the haloarene were found (i.e., biphenyls, phenols, etc.), so we must assume that the reacted haloarenes decompose to volatiles. A second piece of evidence for electrophilic addition was the ipso substitution found for arene **16** in the acetyl position (Scheme 3), which should proceed through an electrophilic aromatic substitution.

We can then conclude that the incorporation of the halide to the arene proceeds by electrophilic aromatic substitution, as occurs for oxyhalogenations in biological systems,[2] and not by radical addition. Furthermore, when 4-methoxystyrene was employed as a substrate, only polyhalogenated products, not alkene oligomers, were found, pointing to X_2 and not to X· as the possible halogenating agent. Polyhalogenated products were exclusively found when styrene, phenylacetylene or 1-decyne was employed as the substrate.

Taking into account the experimental results for halide release and halogenation reactions obtained above, one can propose a

dx.doi.org/10.1021/cs300644s | *ACS Catal.* 2013, 3, 250−258

Scheme 3. Results for the Halogenation of Acetylated Arene 16 (0.0625 mmol) with Tetrachlorethane or 1,3-Dibromopropane 3 (0.75 mL) in the Presence of Nanocrystalline Ceria (0.46 mmol) under an Atmosphere of Oxygen (0.9 mmol) at 140 °C[a]

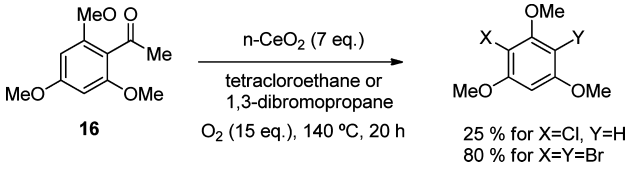

[a]Other chlorinated products were also found.

possible reaction mechanism (Scheme 4). First, oxygen basic species present in nanocrystalline ceria would generate anionic

Scheme 4. Possible Mechanism for the Nanocrystalline Ceria-Mediated Aerobic Oxidative Halogenation of Activated Arenes with Organic Halides

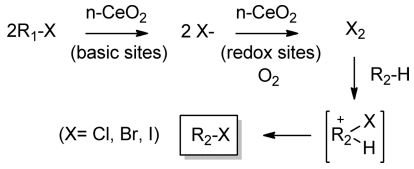

halides from the organic solvent, and then nanocrystalline ceria forms halogen radicals in a redox reaction. Although the former is unaffected by radical scavengers, the latter indeed is, and the oxidative halogenation reaction stops in the presence of 4-*tert*-butyl catechol. Following radical halide formation, as soon as two of these collide to dihalogen species, the arene forms the Wheland intermediate that finally gives the new halogenated molecule by electrophilic aromatic substitution after hydrogen removal. The possible formation of some kind of CeO_2−X intermediate with a partial positive charge instead of X_2 cannot be ruled out.

Concerning the active sites in nanoceria during the catalytic process, kinetic experiments showed that the reaction yield is linearly dependent on the amount of nanoceria (Supporting Information Figure S2), although with a very slow constant (0.35 mmol of product per hour and per equivalent of nanoceria). Temperature-programmed reduction and oxidation of nanoceria showed that most of the redox sites are reduced at temperatures above 350 °C, and only a small fraction (<10%) are affected at the temperature of the oxidative halogenation (~150 °C). These results point to that nanoceria participates in the reaction with only a few sites, which would explain the high amount needed to obtain full conversions.

Scope of the Reaction. The generality of the reaction with respect to the halogenated solvent was studied and the results are given in Table 1.

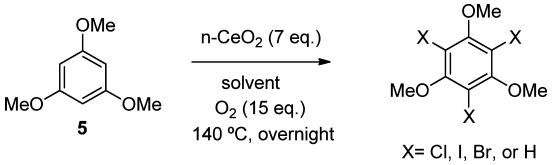

Both alkylic and aromatic bromides, chlorides, and iodides are suitable reagents/solvents for the nanocrystalline ceria-mediated oxidative halogenation of **5** in good yields and with good

Table 1. Results for the Halogenation of 1,3,5-Trimethoxybenzene 5 (0.0625 mmol) with Different Halogenated Solvents (0.5-0.75 mL) in the Presence of Nanocrystalline Ceria (0.46 mmol) under an Atmosphere of Oxygen (0.9 mmol, 6 bar) at 140 °C[a]

Entry	Solvent	Products (yield, %)
1		Dibromochloro (92)
2[a)]		Tribromo (80), dibromochloro (15), bromodichloro (5)
3[b)]		1-bromo (95)
4[c)]		dibromochloro (75), bromodichloro (5), 1-bromo (20)
5		1,3-dibromo (99)
6		1-bromo (80)
7		1-iodo (99)
8		1-chloro (89)
9[d)]		1-chloro (89)
10		1-chloro (79)

[a]GC yields, 100% conversion. [b]HCl (3 equiv) was added. [c]$NaHCO_3$ (3 equiv) was added. [d]H_2O (15 eq. was added). [e]97% conversion.

selectivity. Addition of a Brönsted acid (HCl) improves the degree of halogenation (compare entries 1 and 2), and in contrast, addition of a base ($NaHCO_3$) retards the halogenation (entry 3), in accordance with previous results.[2] Water has a negligible influence on the reaction yield (compare entries 1 and 4). The degree of bromination is solvent-dependent and higher for the alkyl than the aryl bromides (compare entries 1, 5 and 6). Iodination is also possible when a deactivated aryl iodide is used (entry 7), whereas iodobenzene achieved only a 25% yield. Since monochlorination seems to be predominant regardless the nature of the chloride source (entries 8−10), kinetic measurements were performed to evaluate the possible differences in reactivity between alkyl and aryl chlorinated solvents (Figure 6A).

A slightly higher reaction rate in terms of both initial rate and final yield is observed when tetrachloroethane is used as the solvent instead of dichlorobenzene. However, if we consider that tetrachloroethane contains twice the amount of chloride as dichlorobenzene, we must infer that the chlorination process occurs similarly for both alkyl and aromatic halides. The filtration test in hot (Figure 6B) showed no activity from the species in solution, which shows that the controlling step of the chlorination process occurs on the solid surface. The scope of the reaction for different methoxyarenes was also studied (Table 2).

Methyl phloroglucinols, veratrole, and anisole are suitable partners for both chlorination and bromination, giving the corresponding halogenated products **7**−**16** in high yields and selectivity. The halogenation extent can be controlled by either the amount of nanocrystalline ceria or the chemical nature of the solvent (compare entries 5−6 and 12−13). It must be noted that simple halogenated phloroglucinols are themselves an important class of natural products,[26] and for illustration, we selectively

dx.doi.org/10.1021/cs300644s | *ACS Catal.* 2013, 3, 250−258

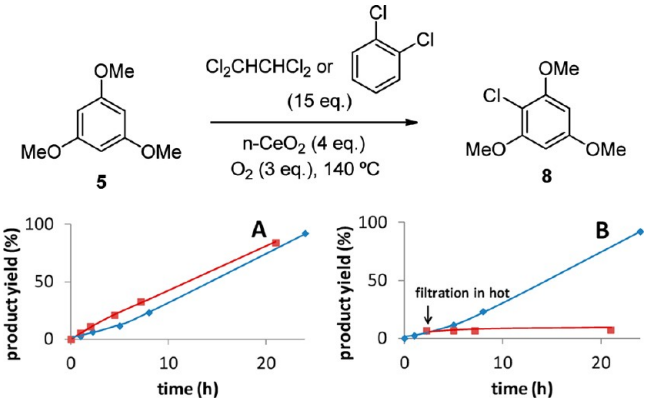

Figure 6. Time−yield plot for (A) halogenation of 1,3,5-trimethoxybenzene **5** (0.32 mmol) with tetracloroethane (□) or *ortho*-dichlorobenzene (◊) in the presence of nanocrystalline ceria (1.2 mmol) under an atmosphere of oxygen (0.9 mmol, 6 bar) at 140 °C, in a reactor equipped with a manometer; (B) halogenation reaction with *ortho*-dichlorobenzene under identical conditions but filtering the solid nanoceria off (□) or not (◊) at the conversion indicated by the arrow. Percentages are with reference to **5**.

demethylated the naturally occurring arene **9**[19] to give the three parent compounds **17**−**19**, the latter also being a natural product (Scheme 5). This synthetic strategy complements the conventional bromination of free phenols.[19,26]

The Role of the Structure of Ceria. At this point, we wanted to know how nanostructurated ceria compares with simple cerium salts as catalysts. In fact, ceric ammonium nitrate (CAN) has been reported as a reagent/catalyst for oxidative halogenations of uracil derivatives with chloride, bromide, iodide salts, and iodine,[27] of alkenes with potassium bromide,[28] and of aromatics with iodine,[29] but the reaction conditions of these chemical systems are not comparable with those here reported. Thus, we have compared the reactivity of nanocrystalline ceria with that of cerium salts and other solid oxides under our typical reaction conditions (Table 3).

The results clearly show that, under the present reaction conditions, only nanocrystalline ceria is active for the chlorination of **5**, and the reaction could be structure-dependent, since no reaction was observed when CeO_2 with relatively low surface (<10 $m^2\ g^{-1}$) area and large particle size (≫10 nm) was used as catalyst (entry 1), and the reaction proceeds very well when CeO_2 is in the form of nanoparticles (<10 nm, entry 2). Iron(III) oxide, also having oxygen vacancies in the structure, is not active for the reaction, regardless the particle size (entries 3−4). Different cerium salts gave a negligible halogenation activity (entries 5−8), and in particular, CAN engages only in the quantitative nitration of **5** (entry 9). All these results illustrate the particular ability of nanocrystalline ceria to generate active halonium species from organic halides and shuttle them to activated arenes under aerobic conditions.

Influence of the CeO_2 Particle Size and Crystal Plane Orientation on the Oxidative Halogenation. Kinetic experiments with different cerium oxides (<10 nm, <25 nm, and <5 μm) were carried out and showed that the smaller the particle size of ceria was, the higher the rate of halide formation (Figure 7A) and, subsequently, the halogenation of **5** was (Figure 7B).

The influence of the ceria particle size on oxidative halogenation activity may suggest that this is a structure-sensitive reaction. Thus, we have synthesized nanocrystals of CeO_2 with different shapes (cubes, octahedra, and rods; see the Experimental section and Figure 6) that preferentially expose the 100, 110, and 111 planes, respectively. Then, the oxidative halogenation of **5** was studied with the three catalysts. The comparative kinetic results are given in Figure 8.

When the initial rate of the halogenation was plotted vs the surface area of the nanocerias (see Figure 8), it could be seen that there is a nonlinear increase when increasing the surface area, again suggesting that crystallite size is not the only factor determining the activity of CeO_2, but atoms with insaturations, in different plane orientations (see the higher intrinsic activity of crystal rods) (or both) can also play an important role in the catalytic halogenation reaction. In accordance with this, it has been very recently reported that ceria nanorods promote the iodination of aromatic compounds with iodine and H_2O_2.[30]

Table 2. Results for the Halogenation of Different Methoxyarenes (0.0625 mmol) with Different Solvents (0.5-0.75 mL) in the Presence of Nanocrystalline Ceria (0.46 mmol) under an Atmosphere of Oxygen (0.9 mmol, 6 bar) at 140 °C[a]

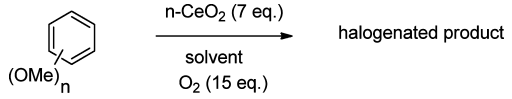

Entry	Arene	Solvent	Main Product (yield, %)
1	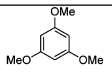		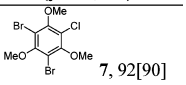 **7**, 92[90]
2			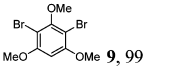 **9**, 99
3			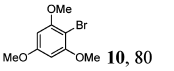 **10**, 80
4			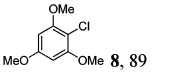 **8**, 89
5[a,b]			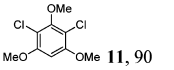 **11**, 90
6[a,b]			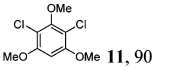 **11**, 90
7	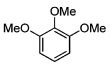		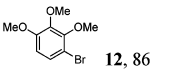 **12**, 86
8[a]			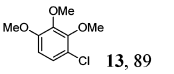 **13**, 89
9[a]			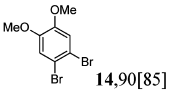 **14**,90[85]
10[a,b]			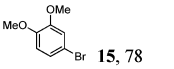 **15**, 78
11[a,b]			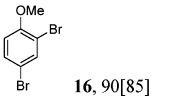 **16**, 90[85]

[a]GC yields. Between brackets, isolated yields. [b]Double amount of nanocrystalline ceria. [c]Half a mount of arene.

dx.doi.org/10.1021/cs300644s | *ACS Catal.* 2013, 3, 250−258

Scheme 5. Selective Demethylation of the Naturally Occurring Arene 9 To Provide the Three Parent Compounds 17−19[a]

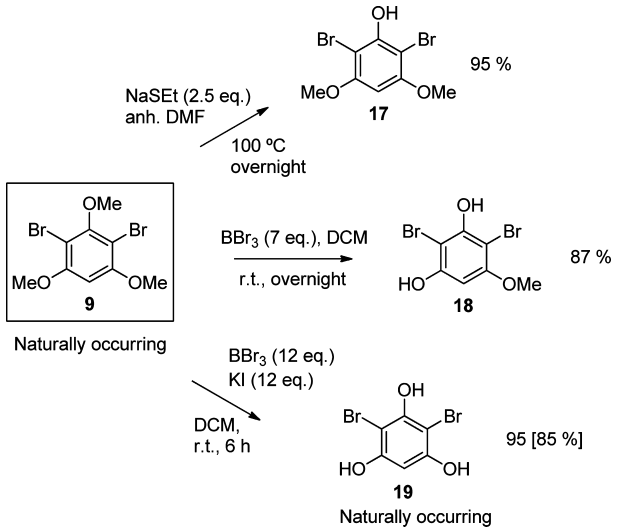

[a]NMR yields, isolated yield under brackets.

Table 3. Results for the Halogenation of 1,3,5-Trimethoxybenzene 5 (0.0625 mmol) with 1,2-Dichlorobenzene (0.75 mL) in the Presence of Different Inorganic Solids under an Atmosphere of Oxygen (0.9 mmol, 6 bar) at 140 °C

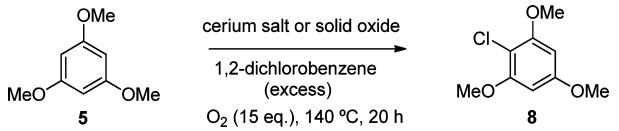

entry	cerium salt or solid oxide	amount (equiv)	product (yield, %)
1	CeO_2	7	0
2	nanocrystalline ceria	7	89
3	Fe_2O_3 (goethite)	10	0
4	nano-Fe_2O_3 (goethite)	10	0
5	$Ce_2(SO_4)_3$	0.3	0
6	$Ce(SO_4)_2{\cdot}4H_2O$	0.3	0
7	$CeCl_3{\cdot}7H_2O$	0.4	0
8	$Ce(NO_3)_3{\cdot}6H_2O$	0.4	<5[a]
9	$Ce(NH_4)_2(NO_3)_6$	0.4	<5[a]

[a]~40% yield of nitroarene.

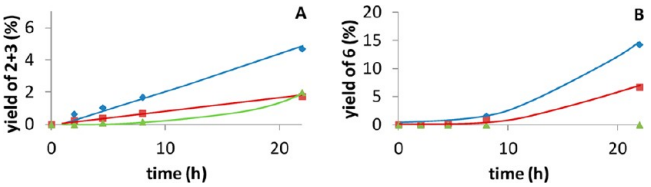

Figure 7. Time−yield plot for the halogen exchange of deaereated 1-bromo-3-chloropropane **1** (A, 40 mmol) or halogenation of 1,3,5-trimethoxybenzene **5** (B, 0.125 mmol) under argon at 140 °C in the presence of 0.46 mmol of <10 nm nanocrystalline (◊), <25 nm (□) or <5 μm ceria (Δ). For the reaction equation, see Scheme 2.

Oxidative Halogenation with Inorganic Halides. Of interest is that the use of simple halide salts as halogen donors and nanocrystalline ceria also activates inorganic iodides, bromides, and chlorides for the oxidative halogenation of **5** (Table 4).[31]

The oxidative halogenation of **5** proceeds well with HBr, LiBr, and KBr as the bromide source, and solvents within a wide range of polarities are suitable for the reaction (entries 1−10). However, the degree of bromination varies as a function of the bromide source and the solvent employed. In general, HBr is more active than LiBr (compare entries 2−3 and 7−8), and the activity decreases as the polarity of the solvent increases (compare entries 6−9). As expected, the corresponding inorganic sources of iodide (entry 11) and chloride (entry 12) are less active. These results show the benefit on reactivity for simple chlorinated and iodinated solvents with respect to the corresponding salts.

Reuse of Nanocrystalline Ceria. The reusability of the nanocrystalline ceria was tested after recovering the solid by simple filtration and recycling for a new reaction. Visually, a change of color in the solid from pale yellow to red is observed (see Reflectance Diffuse (RD) UV−vis spectra in Supporting Information Figure S3), and this was accompanied by the disappearance of the typical peak of CeO_2 in Raman spectroscopy at ~500 cm^{-1} (Supporting Information Figure S4), together with a progressive decrease in the reactivity (Figure 9). Hydrogenation of the reused solid (10 bar H_2, 140 °C, 3 h), before reaction, does not improve the final result. However, when the catalyst was calcined at 500 °C in air, the original CeO_2 structure was restored, as assessed by RD-UV−vis and RAMAN spectroscopy (Supporting Information Figure S4), and a slight increase in the catalytic activity was observed (cycle 6, Figure 9).

Raman spectroscopy also suggests a progressive substitution of oxygen with chloride during reaction that is easily inverted after calcination in air. To check this, X-ray photoelectron spectroscopy (XPS) measurements of the fresh, used, and calcined nanocrystalline ceria were carried out, and the results confirmed the presence of chlorine in the used catalyst and the decrease in halogen after calcination in air (Supporting Information Figure S5). With these data in hand, it seems plausible that chloride is progressively incorporated into the ceria during the reaction and poisons the catalyst, but a simple calcination in air removes part of the halogen and restores the catalytic activity. TEM measurements confirm the robustness of the nanocrystalline ceria structure throughout uses and calcinations, though some sintering of the nanoceria crystals was observed (Figure 10). Therefore, further studies directed to optimize the regeneration conditions will be necessary.

CONCLUSIONS

Nanocrystalline ceria generates active halogenating species from simple organic halides or inorganic acids and salts under aerobic conditions. The process can be engaged with electrophilic aromatic substitutions to overall give the oxidative halogenation of arenes. This methodology provides a simple way to obtain aryl halides from halogenated solvents or salts.

EXPERIMENTAL SECTION

Typical Procedure for Kinetic Experiments at Atmospheric Pressure. Nanocrystalline ceria (80 mg, 0.46 mmol) and 1,3,5-trimethoxybenzene **5** (105 mg, 0.625 mmol) were placed in a 10 mL vial equipped with a magnetic bar, and the vial was sealed with a rubber septum. A stream of argon (or oxygen) was passed over several minutes, and the argon (oxygen) atmosphere was finally preserved with a balloon (~1−1.5 atm). Then the corresponding (deaereated) solvent **1** (0.75 mL) was added, and the resulting mixture was placed in a preheated oil bath at 140 °C

dx.doi.org/10.1021/cs300644s | ACS Catal. 2013, 3, 250−258

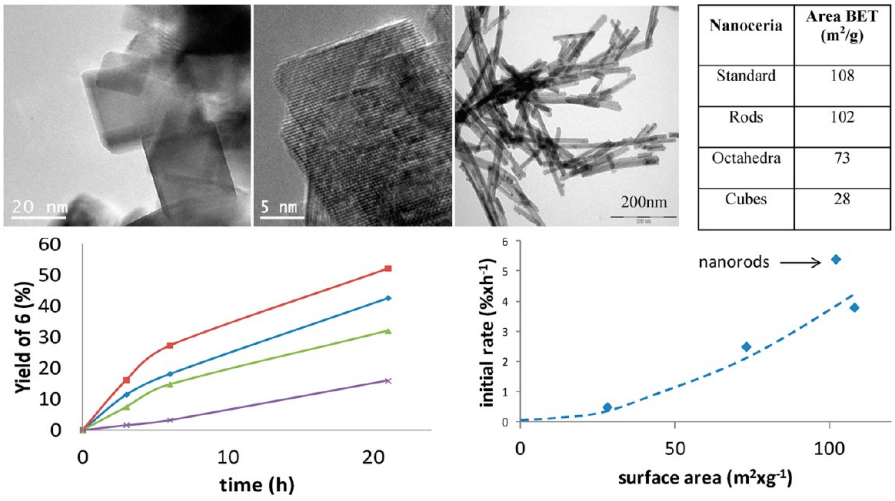

Figure 8. High resolution transmission electron microscopy (HR-TEM) images for ceria nanocubes (top left), nanooctahedra (top center), and nanorods (top right). Top right: typical surface areas for the different nanocerias employed as catalysts. Bottom left: Time−yield plot for the halogenation of 1,3,5-trimethoxybenzene **5** (0.62 mmol) in 1-bromo-3-chloropropane **1**, under oxygen (6 bar, 0.9 mmol) at 140 °C in the presence of 1.2 mmol of ceria nanorods (□), standard nanocrystalline ceria (◊), nanooctahedra (Δ), or nanocubes (×). For the reaction equation, see Scheme 2. Bottom right: Variation of the initial rate as a function of the surface area. Line is a guide to the eyes.

Table 4. Results for the Halogenation of 1,3,5-Trimethoxybenzene 5 (0.0625 mmol) with Bromide and Chloride Salts and Acids (0.125 mmol) in the Presence of Nanocrystalline Ceria (0.46 mmol) under an Atmosphere of Oxygen (0.9 mmol, 6 bar) at 140 °C in Different Solvents (0.75 mL)

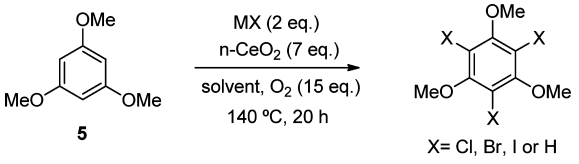

entry	MX	solvent	products (yield, %)
1	HBr	decane	1,3-dibromo (80); 1-bromo (20)
2[a]		*o*-xylene	1,3-dibromo (95)
3		$Cl_2C{=}CCl_2$	tribromo (40); dibromochloro (40); bromodichloro (10)
4		DMF	1-bromo (98)
5[b]		water	1-bromo (48)
6	LiBr	decane	1,3-dibromo (85)
7[a]		*o*-xylene	1,3-dibromo (40); 1-bromo (60)
8		$Cl_2C{=}CCl_2$	dibromochloro (10); 1-bromo (85); 1-chloro (5)
9		DMF	1-bromo (80)
10[b]	KBr	water	1-bromo (90)
11[b]	KI	water	1-iodo (95)
12	LiCl	*o*-xylene	1-chloro (25)

[a]Benzylic oxidation of the solvent was also found. [b]At 100 °C and with 3 equiv of halide.

and magnetically stirred for the indicated time. Aliquots (2−4% of the total volume) were periodically taken, poured into CH_2Cl_2 (1 mL), filtered through a 0.2 μm PTFE filter syringe and subjected to GC and GC/MS analysis after dodecane (11.2 μL, 0.1 mmol) was added as the external standard.

Typical Procedure for Kinetic Experiments under Oxygen Pressure. Nanocrystalline ceria (80 mg, 0.46 mmol), 1,3,5-trimethoxybenzene **5** (105 mg, 0.625 mmol), and 1-bromo-3-chloropropane **1** (0.75 mL) were placed in a double-walled glass 2 mL reactor equipped with a magnetic stirrer and a manometer. The reactor was closed, and oxygen (6 bar, ∼0.9 mmol) was introduced at room temperature. The resulting mixture was placed in a steel heating block at 140 °C and for the indicated time. At the indicated time, the oxygen was measured after cooling and released, and an aliquot (200 μL) of the reaction mixture was taken and poured into CD_3CN (1 mL), filtered through a 0.2 μm PTFE filter syringe, and subjected to ^1H NMR and GC analysis after mesitylene (18.0 μL, 0.13 mmol) was added as the external standard. The reaction mixture was put again under heating after oxygen introduction (6 bar, ∼0.9 mmol) at room temperature.

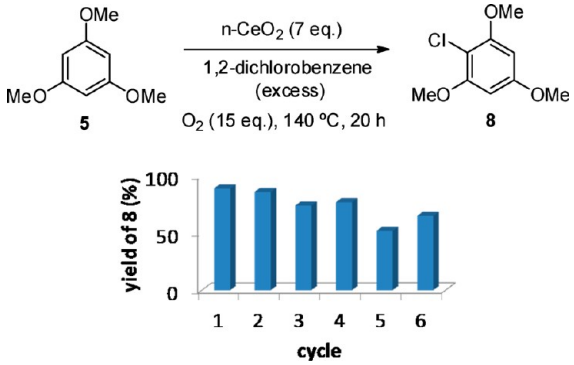

Figure 9. Reuses of nanocrystalline ceria (1.2 mmol) for the chlorination of 1,3,5-trimethoxybenzene **5** (0.062 mmol) with *ortho*-dichlorobenzene under an atmosphere of oxygen (0.9 mmol, 6 bar) at 140 °C.

Typical Procedure for Reactions under Oxygen Pressure. Nanocrystalline ceria (80 mg, 0.46 mmol), 1,3,5-trimethoxybenzene **5** (10.5 mg, 0.0625 mmol), and the corresponding solvent (0.75 mL) were placed in a double-walled glass 2 mL reactor equipped with a magnetic stirrer and a manometer. The reactor was closed, and oxygen (6 bar, ∼0.9 mmol) was introduced at room temperature. The resulting mixture was placed in a preheated oil bath or steel heating block at 140 °C and for the indicated time. After cooling, CH_2Cl_2 (1 mL) was added, and the mixture was magnetically stirred for 1−2 min at room temperature. The final suspension was filtered

dx.doi.org/10.1021/cs300644s | *ACS Catal.* 2013, 3, 250−258

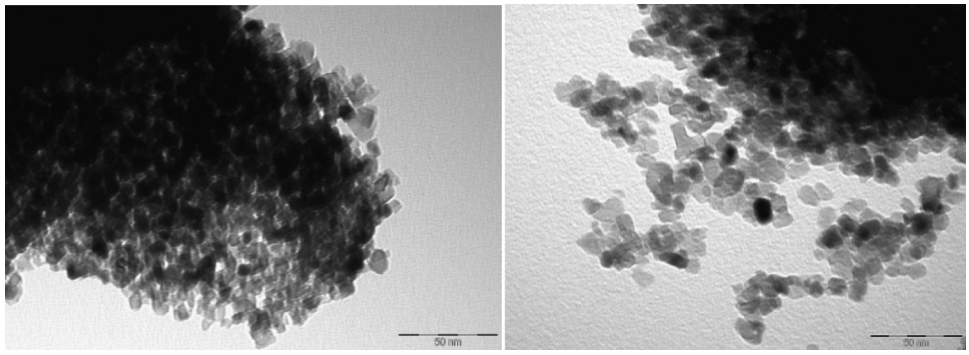

Figure 10. Transmission electron spectroscopy images of nanocrystalline ceria before (left) and after use and calcination under air at 500 °C (right). The particle size average is 8.8 and 10.0 nm, respectively.

through a 0.2 μm PTFE filter syringe and subjected to GC and GC/MS analysis after dodecane (11.2 μL, 0.1 mmol) was added as the external standard. For isolated products, solvents were removed under pressure after filtration to give the resulting products in high purity as assessed by ^{1}H and ^{13}C NMR spectroscopy and MS/GC.

Synthesis of 17. 2,4-Dibromo-1,3,5-trimethoxybenzene **9** (17 mg, 0.05 mmol) and sodium thioethoxide (11 mg, 2.5 equiv) were placed in a dried 10 mL round-bottomed flask equipped with a magnetic stirrer. The flask was capped with a rubber septum, and nitrogen atmosphere was set. Anhydrous dimethylformamide (0.25 mL) was added, and the resulting mixture was placed in a preheated oil bath at 100 °C and magnetically stirred overnight. After cooling, CH_2Cl_2 (0.5 mL) was added, and the mixture was treated with HCl (5 N, 0.5 mL) and neat water (0.5 mL). After solvent removal of the organic phases, the resulting crude was analyzed by ^{1}H NMR and MS/GC.

Synthesis of 18. 2,4-Dibromo-1,3,5-trimethoxybenzene **9** (17 mg, 0.05 mmol) was placed in a 2 mL glass vial equipped with a magnetic stirrer. Then anhydrous CH_2Cl_2 (0.25 mL) and BBr_3 (1 M solution in CH_2Cl_2, 350 μL, 0.35 mmol) were added, and the resulting mixture was magnetically stirred at room temperature overnight. CH_2Cl_2 (0.5 mL) and water (0.5 mL) were added, and the organic phases were separated. After solvent removal, the resulting crude was analyzed by ^{1}H NMR and MS/GC.

Synthesis of 19. 2,4-Dibromo-1,3,5-trimethoxybenzene **9** (34 mg, 0.1 mmol) and KI (200 mg, 1.2 mmol) were placed in a 2 mL glass -vial equipped with a magnetic stirrer. Then, anhydrous BBr_3 (1 M solution in CH_2Cl_2, 1.2 mL, 1.2 mmol) was added, and the resulting mixture was magnetically stirred at room temperature for 6 h. After this time, the mixture was slowly diluted with EtOH (30 mL), and solid $NaHCO_3$ was added after bubbling ceased. The resulting mixture was filtered, the volatiles were removed under vacuum, and the resulting crude was redissolved in CH_2Cl_2 (10 mL) and filtered again. After solvent removal, $CDCl_3$ (0.75 mL) was added, and the solution was filtered again, the filtrates being analyzed by ^{1}H NMR and MS/GC. Solvent removal yielded 25 mg (85%) of **19** as a pale red solid.

Hot Filtration Test. Nanocrystalline ceria (200 mg, 1.2 mmol), 1,3,5-trimethoxybenzene **5** (52.5 mg, 0.32 mmol) and *ortho*-dichlorobenzene (0.75 mL) were placed in a double-walled glass 2 mL reactor equipped with a magnetic stirrer and a manometer. The reactor was closed, and oxygen (6 bar, ~0.9 mmol) was introduced at room temperature. The resulting mixture was placed in a steel heating block at 140 °C and followed by periodically taking aliquots and analyzing them by GC (see above for analysis protocol). In a parallel reaction and at the indicated time, the solid was filtered through a 0.2 μm PTFE filter syringe in hot after oxygen release, and the filtrates were put again under reaction conditions (140 °C, 6 bar of oxygen), following the reaction by GC.

Reuses of Nanocrystalline Ceria. After following the typical reaction protocol under oxygen (see above), the solid was washed three times with CH_2Cl_2 (2 mL), dried at the open air, and weighed, and a second reaction was set with proportional amounts of reactant and solvent at 6 bar of oxygen. After the fifth use, the solid was analyzed by Raman and UV−visible spectroscopy and by XPS. Then it was calcined under ambient conditions at 500 °C for 4 h in a muffle, reanalyzed, and put into a reaction again.

Synthesis of CeO_2 with Different Crystalline Facets. All the reagents used were analytical grade. A solution of NaOH was added under vigorous stirring over a solution of $Ce(NO_3)_3{\cdot}6H_2O$. The formed suspension was kept stirring for 30 min. This milky slurry was transferred to a Teflon liner autoclave, and the autoclave was sealed tightly. The autoclave was transferred in an oven for hydrotermal treatment over 24 h. Table 5 shows the conditions for each type of CeO_2 shape.

Table 5

shape	$V_{Sol.NaOH}/V_{Sol.Ce+3}$	[NaOH] (M)	[Ce^{3+}] (M)	T (°C)
cubes	7	9	0.05	200
octahedra	7	0.01	0.05	175
rods	7	9	0.05	100

After cooling at room temperature, the precipitated yellow-white solids were filtratered and washed thoroughly with distillated water, controlling the pH of the filtrates. After that, the samples were dried at 120 °C under flowing air for 12 h.

■ ASSOCIATED CONTENT

Supporting Information

General details, additional figures, and copies of spectra. This material is available free of charge via the Internet at http://pubs.acs.org.

■ AUTHOR INFORMATION

Corresponding Author

*Phone: +34963877800. Fax: +349638 77809. E-mails: (A.L.-P.) anleyva@itq.upv.es; (A.C.) acorma@itq.upv.es.

Author Contributions

The manuscript was written through contributions of all authors. All authors have given approval to the final version of the manuscript.

Notes

The authors declare no competing financial interest.

■ ACKNOWLEDGMENTS

A.L.-P. thanks CSIC for a contract. D.C.-M. thanks the Spanish MICINN for a postgraduate scolarship (FPI). J.R.C.-A. thanks MCIINN for the concession of a FPU contract. Financial support by Consolider-Ingenio 2010 (proyecto MULTICAT), PLE2009 project from MCIINN, and King Saud University is also acknowledged.

■ REFERENCES

(1) Gribble, G. W. *Acc. Chem. Res.* **1998**, *31*, 141−152.
(2) Podgorsek, A.; Zupan, M.; Iskra, J. *Angew. Chem., Int. Ed.* **2009**, *48*, 8424−8450.
(3) Yonehara, K.; Kamata, K.; Yamaguchi, K.; Mizuno, N. *Chem. Commun.* **2011**, 1692−1694.
(4) Yang, L.; Lu, Z.; Stahl, S. S. *Chem. Commun.* **2009**, 6460−6462.
(5) Trovarelli, A. *Catalysis by Ceria and Related Materials*; Imperial College Press: London, 2002; Vol. *2*.
(6) Pirmohamed, T.; Dowding, J. M.; Singh, S.; Wasserman, B.; Heckert, E.; Karakoti, A. S.; King, J. E. S.; Seal, S.; Self, W. T. *Chem. Commun.* **2010**, 2736−2738.
(7) Rupp, E. C.; Betterton, E. A.; Arnold, R. G.; Sáez, A. E. *Catal. Lett.* **2009**, *132*, 153−158.
(8) de Rivas, B.; López-Fonseca, R.; González-Velasco, J. R.; Gutiérrez-Ortiz, J. I. *J. Mol. Catal. A: Chem.* **2007**, *278*, 181−188.
(9) Gutiérrez-Ortiz, J. I.; de Rivas, B.; López-Fonseca, R.; González-Velasco, J. R. *Appl. Catal., A* **2004**, *269*, 147−155.
(10) Van der Avert, P.; Podkolzin, S. G.; Manoilova, O.; de Winne, H.; Weckhuysen, B. M. *Chem.—Eur. J.* **2004**, *10*, 1637−1646.
(11) Van der Avert, P.; Weckhuysen, B. M. *Phys. Chem. Chem. Phys.* **2004**, *6*, 5256−5262.
(12) Weckhuysen, B. M.; Rosynek, M. P.; Lunsford, J. H. *Phys. Chem. Chem. Phys.* **1999**, *1*, 3157−3162.
(13) Blanco, J.; Ávila, P.; Melo, F. V. *Bull. Chem. Soc. Jpn.* **1983**, *56*, 909−913.
(14) Jun Guo, M.; Varady, L.; Fokas, D.; Baldino, C.; Yu, L. *Tetrahedron Lett.* **2006**, *47*, 3889−3892.
(15) Chen, X.; Hao, X.-S.; Goodhue, C. E.; Yu, J.-Q. *J. Am. Chem. Soc.* **2006**, *128*, 6790−6791.
(16) Barbier, J., Jr.; Delanoë, F.; Jabouille, F.; Duprez, D.; Blanchard, G.; Isnard, P. *J. Catal.* **1998**, *177*, 378−385. (b) Guzman, J.; Carrettin, S.; Corma, A. *J. Am. Chem. Soc.* **2005**, *127*, 3286−3287.
(17) Li, C.; Domen, K.; Maruya, K.-i.; Onishi, T. *J. Am. Chem. Soc.* **1989**, *111*, 7683−7687.
(18) Pirrung, M. C.; Brown, W. L.; Rege, S.; Laughton, P. *J. Am. Chem. Soc.* **1991**, *113*, 8561−8562.
(19) Kiehlmannan, E.; Lauener, R. W. *Can. J. Chem.* **1989**, *67*, 335−344.
(20) Fitzpatrick, L.; Sala, T.; Sargent, M. V. *J. Chem. Soc., Perkin 1* **1980**, 85−89.
(21) Danishefsky, S.; Walker, F. J. *J. Am. Chem. Soc.* **1979**, *101*, 7018−7020.
(22) Shinoda, K.; Yasuda, K. *Chem. Lett.* **1981**, *10*, 1243−1244.
(23) Leseurre, L.; Chao, C.-M.; Seki, T.; Genin, E.; Toullec, P. Y.; Genêt, J.-P.; Michelet, V. *Tetrahedron* **2009**, *65*, 1911−1918.
(24) Borodkin, G. I.; Zaikin, P. A.; Shubin, V. G. *Tetrahedron Lett.* **2006**, *47*, 2639−2642.
(25) Park, C. P.; Nagle, A.; Yoon, C. H.; Chen, C.; Jung, K. W. *J. Org. Chem.* **2009**, *74*, 6231−6236.
(26) Singh, I. P.; Sidana, J.; Bharate, S. B.; Foley, W. J. *Nat. Prod. Rep.* **2010**, *27*, 393−416.
(27) Asakura, J.-i.; Robins, M. J. *J. Org. Chem.* **1990**, *55*, 4928−4933.
(28) Nair, V.; Panicker, S. B.; Augustine, A.; George, T. G.; Thomas, S.; Vairamani, M. *Tetrahedron* **2001**, *57*, 7417−7422.
(29) Das, B.; Krishnaiah, M.; Venkateswarlu, K.; Reddy, V. S. *Tetrahedron Lett.* **2007**, *48*, 81−83.
(30) Zhang, P.; Sun, D.; Wen, M.; Yang, J.; Zhou, K.; Wang, Z. *Adv. Synth. Catal.* **2012**, *354*, 720−729.
(31) Polet, S. *Chem. Tech. (Amsterdam)* **1968**, *23*, 617−620.